Numerical modelling of earth pressure loading of the vertical stem of L-shaped retaining walls

M. Achmus
Institute of Soil Mechanics, Foundation Engineering and Waterpower Engineering, University of Hannover, Germany

ABSTRACT: The influence of system and boundary conditions on the earth pressure acting on the vertical stem of a L-shaped retaining wall is analysed with a numerical model. It is found that only in rare cases, namely with very high wall and subsoil stiffnesses, is the design load due to German regulations reached. In most cases the earth pressure is significantly lower than the average of active earth pressure and earth pressure at rest. A connection is found between the average rotation of the vertical wall stem and the magnitude of the earth pressure load. On this basis a concept for a more sophisticated, but still simple-to-use new design method is outlined.

1 INTRODUCTION

L-shaped walls are simple to construct and thus often used as earth retainment constructions. Since the usual approaches of the design for overall stability (e. g. bearing capacity, sliding) are believed to be reliable and sufficiently accurate, questions remain concerning the magnitude of the earth pressure acting on the vertical stem of the wall (Fig. 1).

For the overall stability design a substitute retaining wall is usually considered This consists of the wall itself and the soil behind the stem and above the wall base. Active earth pressure is assumed to act on the virtual wall back, progressing upwards from the heel of the foundation. The angle of wall friction δ is to set equal to the inclination of the backfill surface β. The assumption of active earth pressure is justified even if the wall deformations in service are small, since before reaching the failure state larger deformations would occur.

In contrast to this, the actual earth pressure load acting in service has to be applied for the design of the vertical wall stem. Due to the existence of the horizontal base it is to be assumed that at least in the lower part of the wall an earth pressure larger than the active earth pressure is effective. To account for this, in the old German regulation DIN 4085 of 1987 a trapezoid distribution of the earth pressures had to be assumed, which leads to an increase of the design wall bending moments when compared with the classical triangular earth pressure distribution.

The actual magnitude and distribution of the earth pressure on the vertical stem is not generally clarified, see, for example, Arnold (2001). Due to the current German regulation DIN 4085 the average of active earth pressure and earth pressure at rest (in the following called increased earth pressure) is to be applied in classical (triangular) distribution. Here the angle of wall friction δ is to set equal to the surface inclination β. Thus the following earth pressure coefficients apply:

$$k_{ah} = \frac{\cos^2 \varphi'}{\left(1 + \sqrt{\frac{\sin(\varphi'+\beta)\sin(\varphi'-\beta)}{\cos^2 \beta}}\right)^2} \tag{1}$$

$$k_{oh} = \frac{\sin \varphi' - \sin^2 \varphi'}{\sin \varphi' - \sin^2 \beta} \cos^2 \beta \tag{2}$$

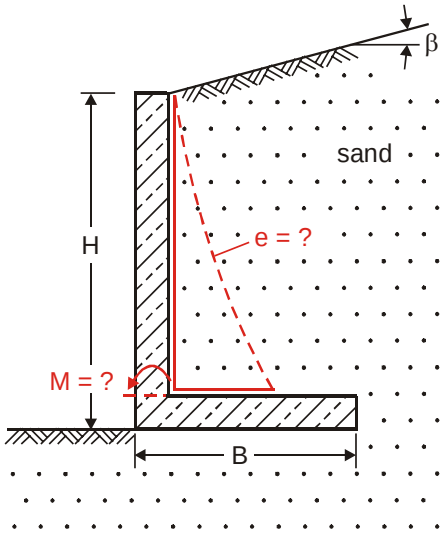

Figure 1. Schematic sketch of a L-shaped retaining wall.

Considering this, the maximum wall bending moment M at a depth z below the wall top due to the soil dead weight amounts to

$$M(z) = \frac{1}{6}\gamma z^3 \frac{1}{2}\left(k_{ah} + k_{0h}\right) \quad (3)$$

On the basis of numerical investigations Goh (1993) proposed to apply active earth pressure in the upper half of the wall and to increase the pressure in the lower half from the active value in the middle of the wall to increased earth pressure for rough walls, or earth pressure at rest for smooth walls at the bottom. This leads to lower bending moments compared to the current German regulation approach.

It is obvious that the wall displacements, and therefore the actual earth pressure magnitude, is dependent on the wall geometry (height H, width B or ratio B/H), the wall stiffness and the stiffnesses of the backfill and the subsoil material (see Achmus & Rouili 2004, Arnold 2004). In this paper the influences of these parameters are quantified by numerical modelling. On this basis, a concept for a new design method is outlined.

2 NUMERICAL MODELLING

The Plaxis programme code (Brinkgreve & Vermeer 2002) was used for the numerical modelling. Medium dense sand is considered as backfill material. Since the dependence of the earth loading on the wall deformations is to be analysed, an accurate consideration of the stress-deformation behaviour of sand is very important.

2.1 *Material law for sand*

The Hardening Soil (HS) material law implemented in the Plaxis code is applied (see Schanz et al. 1999). This elastoplastic material law accounts in a realistic manner for the stress-dependence of the soil stiffness for oedometric and deviatoric stress paths as well as for unloading and reloading states. Using three reference stiffness modules and a parameter m as input parameters, the stress-dependency is modelled as follows (here cohesion is set to zero):

$$E_{(\sigma_3)} = E_{ref}\left(\frac{\sigma_3}{\sigma_{ref}}\right)^m \quad (4)$$

The reference stiffness modulus $E_{oed,ref}$ is determined by oedometer tests, and the modules $E_{50,ref}$ and $E_{ur,ref}$ are determined in conventional triaxial tests by loading and un-/reloading, respectively.

With two yield surfaces shear hardening as well as compression hardening is accounted for. The shear yield surface is of the Mohr-Coulomb type. Plastic deformations are determined via a non-associated flow rule with a dilatancy angle ψ. The failure surface is defined by the shear parameters, i.e. angle of internal friction φ' and cohesion c'. Plastic deformations at oedometric stress paths are determined using a cap yield surface with associated flow rule. For a detailed description of the Hardening Soil (HS) material law reference is made to Schanz et al. (1999).

Beside the unit soil weight γ a total of seven parameters are necessary to describe the stress deformation behaviour of the soil. For the numerical calculations presented in the following, the parameters typical for a medium dense sand given in Table 1 have been used.

Table 1. Parameters of the Hardening Soil (HS) material law used for medium dense sand.

Unit weight:	γ = 17 kN/m^3
Stiffness parameters (σ_{ref} = 100 kN/m^2):	$E_{oed,ref}$ = 25 MN/m^2
	$E_{50,ref}$ = 25 MN/m^2
	$E_{ur,ref}$ = 100 MN/m^2
	m = 0.65
Shear parameters:	φ' = 35°
	c' = 0
	ψ = 2.5°

2.2 *Validation*

For the validation of the material law chosen, the deformation dependency of earth pressure acting on a rigid wall was modelled. For this problem, comparisons with experimental results documented in the literature are possible.

In the upper part of Fig. 2 the system modelled is shown schematically. A wall with a height of 5 m was considered. The soil behind the wall was applied in 5 steps in layers of 1 m thickness. Between wall and soil an interface was defined with a maximum wall friction angle of δ = 29.3°. The wall movement was controlled by the stiffness of two anchor elements supporting the wall. The stiffnesses were in each case chosen in such a way that a combination of translatoric and rotational movement of the rigid wall occurred. In the lower part of Fig. 2 the earth pressure distributions obtained with three different displacement modes (θ = wall rotation angle) are shown.

As assumed, an approximately linear increase of the earth pressure is obtained with depth. The coefficient of horizontal earth pressure can be determined by the following equation:

$$k_h = \frac{E_h}{0.5\gamma H^2} = \frac{\int_{z=0}^{z=H} e_h \, dz}{0.5\gamma H^2} \quad (5)$$

In Fig. 3 the calculated earth pressure coefficients for the case of a horizontal surface (β = 0) are presented dependent on the wall rotation $tan\ \theta$. From

the at-rest state the earth pressure decreases with increasing wall rotation, reaching a minimum value corresponding to the active state at a rotation of about *tan* θ = 0.5 to 0.6 %.

For the base rotation mode wall rotations between 0.2 and 0.6 %, dependent on the relative density, are usually assumed to be necessary to reach the active limit state in sand, see for example Fang & Ishibashi (1986). For translatoric displacement normally even smaller maximum wall displacements apply. For pure translatoric displacement in medium dense sand, Ishihara et al. (1995) determined a ratio of displacement to wall height of about 0.4 %.

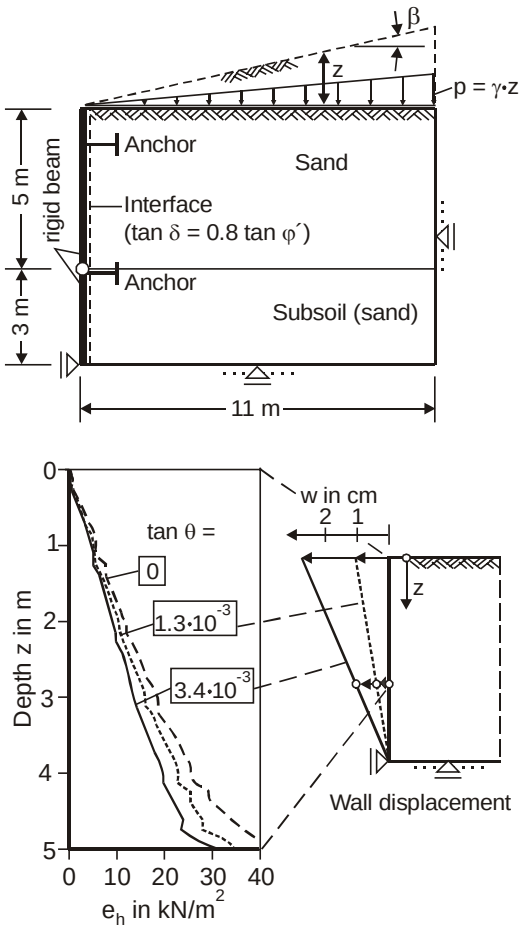

Figure 2. Earth pressure problem. System (top) and earth pressure distributions for different displacement modes (below).

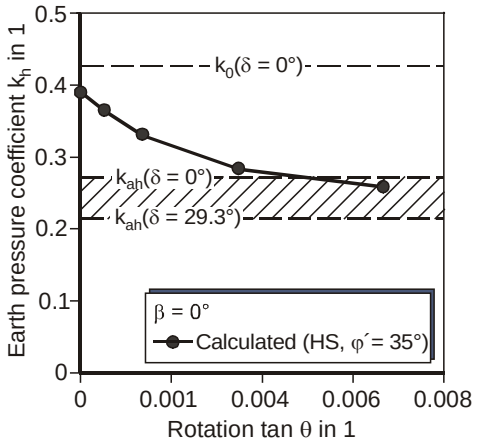

Figure 3. Calculated dependence of the earth pressure coefficient from the wall rotation (surface inclination β = 0).

Altogether, good agreement of the calculated displacement-dependency of the earth pressure with existing experience can be stated. There is a tendency to slightly overestimate the displacement necessary to reach the active state. For the determination of a deformation-dependent earth pressure approach for L-shaped walls, the modelling will thus presumably give results lying on the safe side.

2.3 *Modelling of the L-shaped wall system*

First, an L-shaped wall with a height of 5 m, a base width of 3.25 m (*B/H* = 0.65) and a wall thickness of *d* = 0.4 m is considered as a basic system. The configuration corresponds to the system shown in Fig. 1.

The subsoil was modelled down to a depth of 5 m below the wall base. Medium dense sand was assumed for both backfill and subsoil material. Wall stem and base were modelled by beam elements. Young's modulus of reinforced concrete was assumed with $E_b = 3 \cdot 10^4$ MN/m^2. Elements with a wall friction angle of $\delta = 0.84\ \varphi' = 29.3°$ were applied between wall and soil interface.

In analogy to the earth pressure problem modelling, a stepwise application of the backfill soil in layers of 1 m thickness was simulated.

In Fig. 4 the wall displacement is given together with the earth pressure loading of the vertical stem obtained. In the upper part of the wall the pressure corresponds to active earth pressure, while it increases in the lower part and locally nearly reaches the earth pressure at rest. This general distribution was also obtained in centrifuge tests reported by Djerbib et al. (2001).

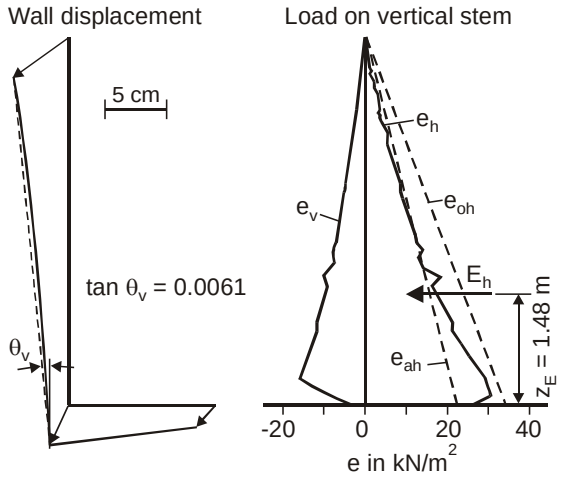

Figure 4. Calculation results for the basic system (*H* = 5 m, *B/H* = 0.65, *d* = 0.4 m).

The resultant load acts at z_E = 1.48 m above the wall toe (z_E/H = 0.30). The earth pressure coefficient calculated with Equation (5) is k_h = 0.301 and is thus about 10% larger than the active earth pressure coefficient for δ = 0 (k_{ah} = 0.271). It is significantly

smaller than the increased earth pressure coefficient of 0.349 which has to be used due to the German regulation. The k_h-value calculated corresponds with a horizontal displacement on the wall top of 4.61 cm and of 1.57 cm on the wall base, which yields an average rotation of the vertical wall stem of *tan* θ_v = 0.0061.

3 PARAMETRIC STUDY

To investigate the connection of the system and boundary conditions and the magnitude of the earth pressure loading of the vertical wall stem, a parametric study was carried out with the numerical model.

In all cases the earth pressure distribution was similar to that shown in Fig. 4. The height of the point of action of the resultant load always lay in the bandwidth $0.29\ H \le z_E \le 0.33\ H$. As a good and conservative approximation, the height of the point of action can be assumed at one third of the wall height, i. e. $z_E \cong 0.33\ H$. In the following only the horizontal earth pressure coefficient is considered as a measure for the magnitude of the earth pressure load and the resultant maximum bending moment of the wall stem.

3.1 *Variation of wall geometry and subsoil stiffness*

First, the width of the wall base B and the wall thickness d, i. e. the stiffness of the wall, was varied for the wall height H = 5 m of the basic system. The results for the earth pressure coefficient k_h are given in Fig. 5 (top).

An increasing coefficient with increasing wall width and increasing wall stiffness is found. Also, a higher width B leads to a lower overall rotation of the wall, and a higher wall stiffness leads to a smaller bending deformation of the vertical wall stem. Thus, both effects reduce the average rotation of the vertical wall stem *tan* θ_v. This dependence is depicted in Fig. 5 (below).

Additionally, the stiffness of the subsoil was varied. For a weak subsoil an oedometric stiffness modulus of E_s = 10 MN/m^2 was assumed, and for a stiff subsoil E_s = 200 MN/m^2. The results (only for d = 0.4 m) are also given in Fig. 5. Again it is found that a stiffness increase leads to an increase of the earth pressure coefficient and to a reduction of the rotation *tan* θ_v.

From the numerical investigation it is found that for the considered wall height of 5 m only in rare cases, namely with very stiff subsoil, very stiff wall and relatively large width of the wall base, does a loading in the magnitude of increased earth pressure originate.

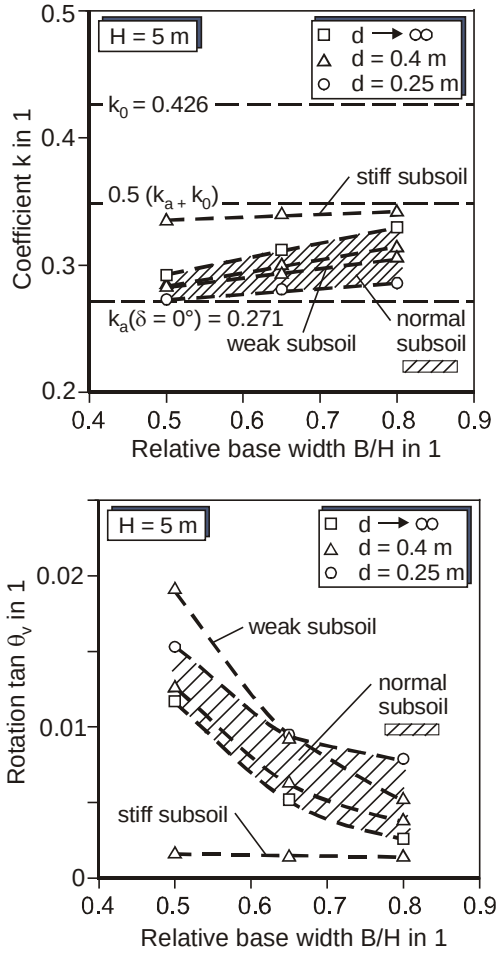

Figure 5. Earth pressure coefficient k_h (top) and average rotation of the vertical stem *tan* θ_v (below) dependent on system and boundary conditions (H = 5 m).

Subsequently, the height of the L-shaped wall was also changed. Results for wall heights of 2 m, 5 m and 9 m are presented in Fig. 6. There is a tendency for small wall heights slightly higher earth pressure coefficients, but with that also smaller wall rotations to arise.

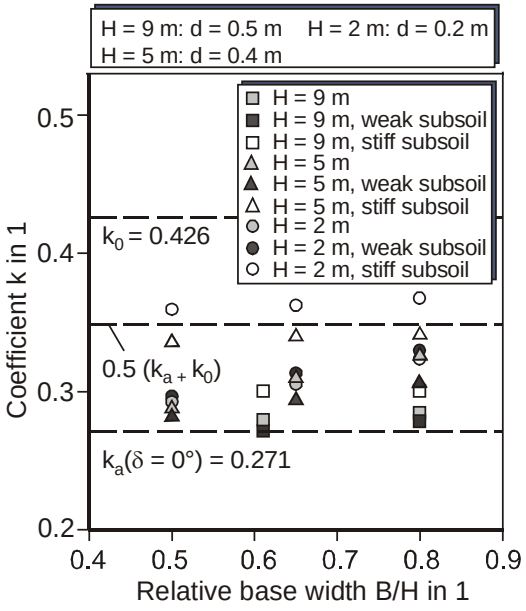

Figure 6. Earth pressure coefficients k_h for H = 2, 5 and 9 m.

The earth pressure coefficient and the average rotation of the vertical stem are influenced by the same parameters. A direct connection between these two values can be presumed. In Fig. 7 the calculated earth pressure coefficients are given dependent on the corresponding wall rotations *tan* θ_v. The results for all wall geometries and subsoil stiffnesses investigated in the parametric study are given with the exception of the unrealistic values obtained with the assumption of a rigid wall ($d \rightarrow \infty$).

A clear dependence of the two values is evident, and this is nearly independent of the system and boundary conditions.

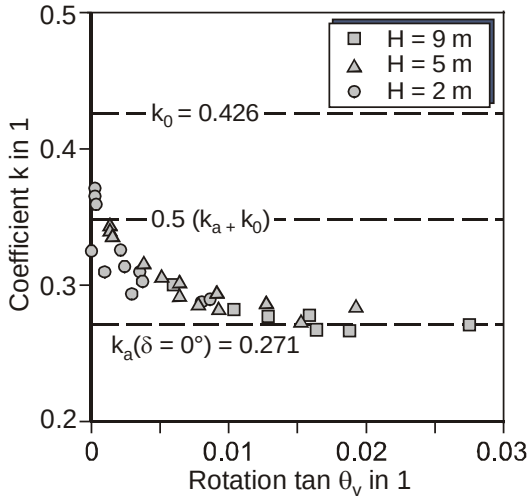

Figure 7. Dependence of the earth pressure coefficient k_h on the average rotation of the vertical stem *tan* θ_v.

3.2 *Variation of surface inclination*

The calculation results presented in section 3.1 are valid for a horizontal surface of the backfill material ($\beta = 0°$, see Fig. 2 top). In a further step the parametric study was extended to surface inclinations $\beta > 0$.

A special problem in this context is to determine the earth pressure at rest in the numerical model. Equation (2) for the coefficient k_{0h} is purely empirical and must thus not necessarily be confirmed in numerical calculations. If a comparison with analytical results should be carried out, the deviations must be taken into account. For this reason the earth pressure problem presented in section 2.2 was also considered for cases with $\beta > 0$.

In a first step the triangular soil block shown in Fig. 2 (top) was applied stepwise in triangular layers. However, with this procedure unrealistically high earth pressures were obtained for the at-rest state (rigid wall and rigid anchors). The reason is a stress redistribution inside the triangular soil block, inducing a concentration of the vertical pressures beneath the wall. To avoid this effect, the surface inclination was considered via a triangular load $p = \gamma z$ acting on the horizontal surface (see Fig. 2 top).

From the exemplary presentation of the deformation-dependence of the earth pressure coefficient for $\beta = 10°$ in Fig. 8 it is evident that this procedure gives realistic results for the earth pressure at rest, i. e. k_{0h}-values comparable with the analytical approaches. There is a tendency for the earth pressure at rest to be slightly overestimated. This trend is the more intensive, the higher the surface inclination β is. This has to be kept in mind in the evaluation of the results for L-shaped walls presented in the following.

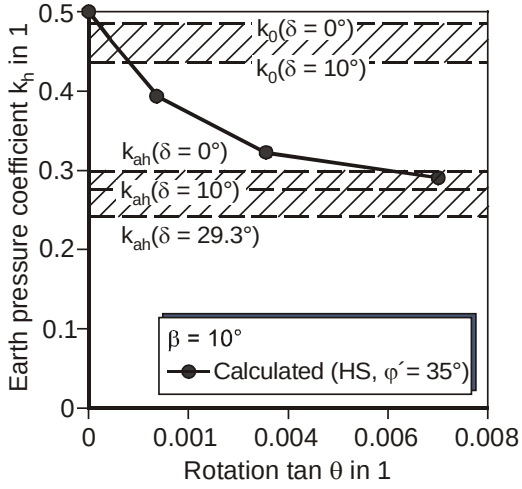

Figure 8. Deformation-dependence of the earth pressure coefficient for $\beta = 10°$.

The same parameter variations presented in section 3.1 for $\beta = 0°$ were carried out for L-shaped walls with surface inclinations of 8°, 15° und 25°. The calculated earth pressure coefficients dependent on the rotation of the vertical wall stem are given in Fig. 9. The analytical earth pressure coefficients determined by Equation (2) are also shown. The connection between k_h and the rotation *tan* θ_v is also confirmed for an inclined surface.

In contrast to the case $\beta = 0$, for $\beta > 0$ with very small wall rotations earth pressure coefficients are obtained which are higher than the increased earth pressure to be applied due to the German regulation DIN 4085. However, the reason for this is the overestimation of the earth pressure at rest compared with the analytical approach discussed above. Taking this into account, it seems reasonable to assume that also for an inclined surface increased earth pressure is the maximum load occurring only in cases with very small wall rotations. In almost all cases a smaller, and from a certain limit rotation, active earth pressure is to be expected.

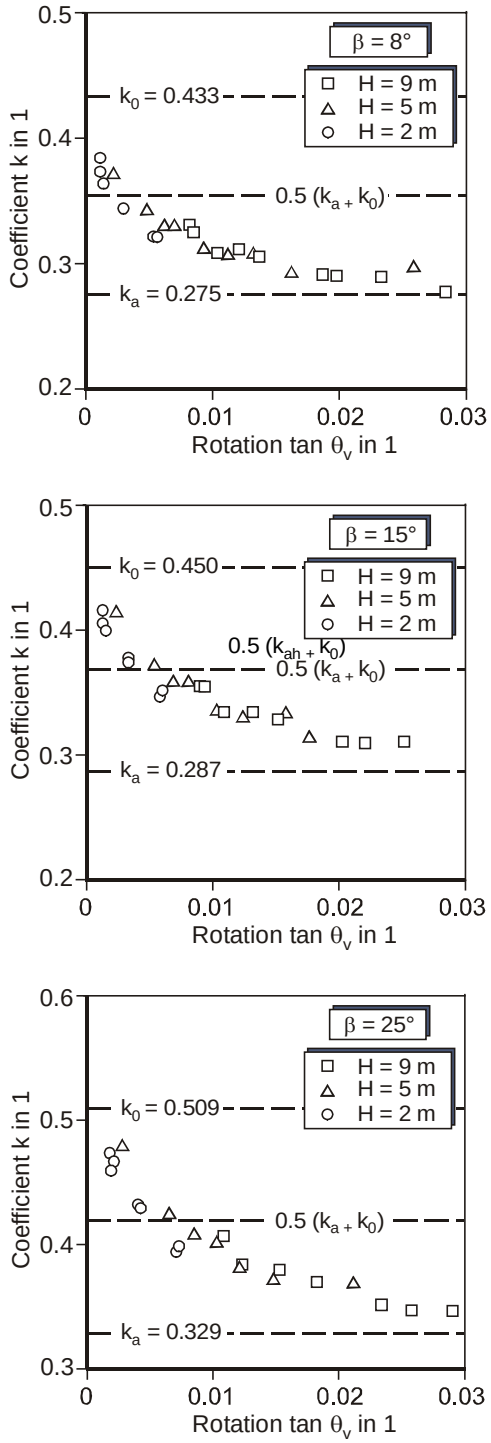

Figure 9. Dependence of the earth pressure coefficient k_h on the average rotation of the vertical stem *tan* θ_v for β = 8, 15 and 25°.

4 CONCLUSIONS

Due to current German regulations the vertical wall stem of L-shaped walls is to be designed for increased earth pressure in classical distribution. The results of the numerical modelling prove that this approach is realistic only for very stiff systems, i. e. very high wall and subsoil stiffnesses. In most cases the loading will therefore be overestimated. Similar results were obtained from Arnold (2004), who also carried out numerical investigations and found that the resultant earth pressure is strongly dependent on the stiffness of the subsoil and the wall width.

A promising design approach results from the determined dependence of the earth pressure coefficient on the average rotation of the vertical wall stem. With a usual settlement calculation and by calculation of the bending deformation of the vertical stem the average rotation can be easily estimated. Dependent on this value, the earth pressure coefficient to be applied can be determined (see also Achmus & Rouili 2004). This new approach is more sophisticated than the old one, but still simple to use.

Due to the calculated results, a wall rotation of *tan* θ_v = 0.01 to 0.015 is necessary to reach the state in which active earth pressure can be applied. Increased earth pressure is to be applied only if *tan* θ_v = 0, and for cases with 0 ≤ *tan* θ_v ≤ 0.01 (0.015) a linear interpolation between these limit values may be carried out.

These results were derived for medium dense sand as backfill material. There is no doubt that the values need verification by experimental tests. But, in combination with experimental results the results of the numerical study can form the basis for a new, and in most cases more economic, design approach for the vertical stem of L-shaped walls.

REFERENCES

Achmus, M. & Rouili, A. 2004. Untersuchung zur Erddruckbeanspruchung von Winkelstützwänden. *Bautechnik* 81, H. 12 (December), pp. 942-948 (in German).

Arnold, M. 2001. Modellversuche zum Erddruck auf Winkelstützwände. In: *Mitteilungen des Instituts für Geotechnik der Universität Dresden*, H. 9, pp. 23-34 (in German).

Arnold, M. 2004. Zur Berechnung des Erd- und Auflastdrucks auf Winkelstützwände im Gebrauchszustand. *Mitteilungen des Instituts für Geotechnik der Universität Dresden*, H. 13 (in German).

Brinkgreve, R.B.J. & Vermeer, P.A. 2002. Plaxis Version 8 (Handbook). Balkema, Rotterdam.

Djerbib, Y., Hird, C.C. & Touahmia, M. 2001. Centrifugal model tests of uniform surcharge loading on L-shaped retaining walls. *15th Int. Conf. on Soil Mechanics and Foundation Engineering, Istanbul*, Vol. 2, pp. 1137-1140.

Fang, Y.S. & Ishibashi, I. 1986. Static earth pressures with various wall movements. *Journal of Geotechnical Engineering*, Vol. 112, No. 3, pp. 317-333.

Goh, T.C. 1993. Behaviour of cantilever retaining walls. *Journal of Geotechnical Engineering*, Vol. 119, No. 11, pp. 1751-1770.

Ishihara, K., Arakawa, T., Saito, T., Hada, M. & Huang, Y. 1995. Study on the earth pressure by using a large-size soil box with a movable wall. *Proc. of the 30th Japan National Conf. on SMFE*, pp. 1717-1720 (in Japanese).

Schanz, T., Vermeer, P.A. & Bonnier, P.G. 1999. The hardening soil model: Formulation and verification. In: *Beyond 2000 in Computational Geotechnics – 10 Years of Plaxis*. Balkema, Rotterdam.